

Critical behavior of the Ising model on fractal structures in dimensions between one and two: Finite-size scaling effects

Pascal Monceau^{1,2} and Michel Perreau¹

¹Laboratoire de Physique Théorique de la Matière Condensée, Université Paris 7, 2 Place Jussieu, 75251 Paris Cedex 05, France

²Département de Physique et Modélisation, Université d'Evry-Val d'Essonne, Boulevard F. Mitterrand, 91025 Evry Cedex, France

(Received 28 April 2000; revised manuscript received 12 July 2000; published 19 April 2001)

The magnetic critical behavior of Ising spins located at the sites of deterministic Sierpinski carpets is studied within the framework of a ferromagnetic Ising model. A finite-size scaling analysis is performed from Monte Carlo simulations. We investigate four different fractal dimensions between 1.9746 and 1.7227, up to the sixth and eighth iteration step of the fractal structure in one case. It turns out that the finite-size scaling behavior of most thermodynamical quantities is affected by scaling corrections increasing as the fractal dimension decreases, tending towards the lower critical dimension of the Ising model. These corrections are related to the topology of the fractal structure and to the scale invariance. Nevertheless the maxima of the susceptibility follow power laws in a very reliable way, which allows us to calculate the ratio of the exponents γ/ν . Moreover, the fixed point of the fourth order cumulant at T_c exhibited by Binder on translation invariant lattices is replaced by a decreasing sequence of intersection points converging towards the critical temperature. The convergence towards the thermodynamical limit as the size of the networks increases is slowed down as the fractal dimension decreases. At last, the evolution of the discrepancies between Monte Carlo simulations and ϵ expansions with the fractal dimension is set out.

DOI: 10.1103/PhysRevB.63.184420

PACS number(s): 75.40.Mg, 64.60.Ak, 05.50.+q

I. INTRODUCTION

The problem of criticality on self-similar structures appeared since the early works of Gefen *et al.*¹⁻⁵ The classical ϵ expansions yield critical exponents associated with second order phase transitions in noninteger dimensions. The first question in dealing with this problem is to study the link between these theoretical expansions and physical systems such as fractal materials.⁶ Moreover, we know that translation invariance is a necessary hypothesis to proceed with dimensional perturbation.¹ Since this invariance is broken in noninteger dimensions, the second and main question is the following: how can the scale invariance of the underlying self-similar structure affect a second order phase transition? Following the early works of Gefen, many authors have dealt with these problems by several methods: real space renormalization group,^{1,3,5,7} ϵ expansions,⁸ high-temperature expansions,⁹ Monte Carlo simulations.^{10,7,11,12} They led to controversial results, discussed in Sec. C of the former article of Monceau *et al.*¹³ For instance, the question whether the Hausdorff dimension is the relevant one which can be associated with universality in the case of fractal dimensions between one and two was still opened. The most recent papers on the subject appeared nearly at the same time, using powerful Monte Carlo simulation methods. Monceau *et al.*¹³ used merely the Wolff algorithm together with the histogram method, whereas Carmona *et al.*¹⁴ used Wolff and Metropolis algorithms together with the spectral density method. In this way, the two groups were able to study the critical behavior much more thoroughly. They noticed that the computation of critical exponents, using the finite size scaling analysis comes up against a main difficulty: scaling corrections appear to be very strong. Indeed, they are stronger on

fractal lattices than on two-dimensional quasiperiodic ones,¹⁷ which are another case of lattices without translation invariance. A similar result was obtained in an analytic way by Liu¹⁵ in the particular case of the Sierpinski gasket. Nevertheless, this result cannot be directly related to the problem we are dealing with, since no phase transition in the thermodynamical limit occur in the case of the gasket. (In other words, an infinitely narrow transition occurs right at $T=0$.) As a matter of fact, a full understanding of second order phase transitions in fractals needs the investigation of dimensions higher than 2. Very recently, Hsiao *et al.*¹⁶ studied three fractal dimensions between 2 and 3. They showed that scaling corrections vanish much more quickly than in the present case, and were able to give evidence that the hyperscaling relation is satisfied when the space dimension is replaced by the Hausdorff one. Indeed, second order phase transitions at nonzero temperature occur at the both integer bounds, while we study here dimensions between the lower critical dimension of the Ising model and two.

In this paper, we investigate four different fractal dimensions in order to show how the scaling corrections can be related to the convergence speed of the thermal averages towards the infinite limit as the size of the lattice increases. We give evidence that this speed decreases as the fractal dimension is lowered. Static critical exponents will be calculated when the lattice sizes we can simulate enable us to reach properly the region where corrections vanish; otherwise, bounds will be given. This article is divided into three parts: the model, the numerical methods, and the scaling theory are briefly recalled in Sec. II. Numerical results associated with the four fractal dimensions we studied are set out in Sec. III. Section IV is devoted to a synthetic discussion in the light of our recent simulations and the results of Carmona *et al.*

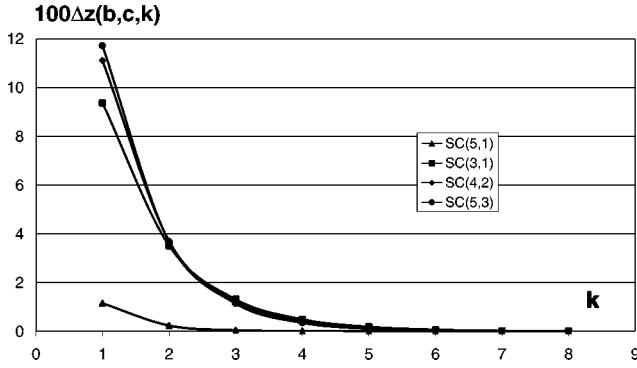


FIG. 1. The behavior of the relative deviation of the mean number of first neighbors $\Delta z(b,c,k)$ versus the segmentation step k .

II. THE METHODS

A. The fractal structure and the magnetic model

The fractal structures we deal with are deterministic Sierpinski carpets.¹⁸ They are constructed in the following way: a square is segmented into b^2 subsquares, and c^2 subsquares are deleted in the center of the initial square. This segmentation process is iterated on the remaining subsquares k times. We shall call $SC(b,c)$ the mathematical fractal, obtained in the limit where k tends towards infinity, and $SC(b,c,k)$ the structure associated with a finite number of segmentation steps. The fractal dimension reads $d_f = \ln(b^2 - c^2)/\ln(b)$. The mean number of first neighbors per site $\langle z(b,c,k) \rangle$ is a convenient measure of the mean local topology of a given network $SC(b,c,k)$; transfer-matrix methods enable us to calculate $\langle z(b,c,k) \rangle$ analytically.¹⁹ In the case of periodic boundary conditions, they yield

$$\langle z(b,c,k) \rangle = \frac{4(b^2 - c^2 - b - c)}{b^2 - c^2 - b} + \frac{4c}{b^2 - c^2 - b} \left(\frac{b}{b^2 - c^2} \right)^k. \quad (1)$$

The relative deviation $\Delta z(b,c,k)$ from the infinite limit thus reads

$$\Delta z(b,c,k) = \frac{\langle z(b,c,k) \rangle - \langle z(b,c,\infty) \rangle}{\langle z(b,c,\infty) \rangle}. \quad (2)$$

The behavior of $\Delta z(b,c,k)$ versus k is given in Fig. 1, for the four Sierpinski carpets studied in the present paper. They have an infinite ramification order which means that one must cut an infinite number of bonds to isolate any bounded part of the fractal. Thus, these fractals are entirely connected, which implies the existence of a second order ferromagnetic Ising transition at finite non zero temperature.⁵ The spins $\frac{1}{2}$ are located at the sites of the deterministic Sierpinski carpet, and the Hamiltonian reads

$$H = -J \sum_{\langle i,j \rangle} s_i s_j. \quad (3)$$

s_i assume the values ± 1 and the summation runs on all interacting first neighbor pairs. The exchange coupling constant J is assumed to be positive.

B. The numerical methods and the standard finite size scaling analysis

The Monte Carlo simulations have been carried out using the Wolff algorithm.²⁰ The use of the single histogram method^{21,22} to process the data obtained from a Monte Carlo simulation at a given temperature T_0 allowed us to calculate the thermodynamical averages over a range ΔT around T_0 . Given a fractal structure $SC(b,c,k)$, we call $L = b^k$ the linear size of the lattice, and $N = (b^2 - c^2)^k$ the number of spins. $\langle E \rangle_T$ and $\langle M \rangle_T$ are the canonical thermodynamical averages of the total energy and the absolute value of the magnetization at temperature T . $m(L,T) = (1/N) \langle M \rangle_T$ is the associated magnetization per spin. The specific heat $C(L,T)$ and the zero field magnetic susceptibility $\chi(L,T)$ per spin are thus given by

$$C(L,T) = \frac{1}{N} \frac{\langle E^2 \rangle_T - \langle E \rangle_T^2}{k_B T^2}, \quad (4)$$

$$\chi(L,T) = \frac{1}{N} \frac{\langle M^2 \rangle_T - \langle M \rangle_T^2}{k_B T}. \quad (5)$$

The standard finite size scaling analysis, developed by Fisher,^{23,24} provides a powerful tool to determine the critical exponents from the behavior of the thermodynamical averages as a function of the size of the system.²⁵ According to the standard scaling hypothesis, and provided that the size of the system is large enough, we can write, right at the critical point $C(L,T_C) \sim L^{\alpha/\nu}$, $\chi(L,T_C) \sim L^{\gamma/\nu}$, and $m(L,T_C) \sim L^{-\beta/\nu}$, where ν is the correlation length exponent. The computation of the critical exponents α , β , γ , can be deduced from the size dependence of the thermodynamical averages, provided that T_C and ν are known with a sufficient accuracy. In a general way, scaling corrections are appreciable when L is not large enough, and they can be described by an additional exponent ω . The above power laws must be replaced by relations under the following form (for instance, in the case of the susceptibility): $\chi(L,T_C) \sim L^{\gamma/\nu} (1 + A_\chi L^{-\omega})$. A_χ is the amplitude of the corrections related to χ .

It is worth noticing that this standard analysis has to be slightly modified if α is strictly negative. In that case, the divergence of the specific heat at the critical point in the thermodynamic limit is replaced by a hump. For finite-sized systems, we should write $C(L,T) = C_\infty(t) + L^{\alpha/\nu} \mathcal{C}(tL^{1/\nu})$, where $t = (T - T_C)/T_C$ is the rescaled deviation from the critical temperature, and \mathcal{C} is a scaling function with $\mathcal{C}(0)$ negative.

Furthermore, finite size effects replace the divergences at the critical point by finite peaks, shifted away from T_C . Effective critical temperatures can thus be defined, for each size and each physical quantity concerned, as the positions of these maxima. ν can be calculated, without knowing T_C by looking at the size dependence of the peaks in the logarithmic derivatives of M^n ($\beta_B = 1/k_B T$):

$$\phi_n(L,t) = \frac{\partial \ln(\langle M^n \rangle_T)}{\partial \beta_B} = \langle E \rangle_T - \frac{\langle EM^n \rangle_T}{\langle M^n \rangle_T}. \quad (6)$$

Assuming that the logarithmic derivatives of M^n fulfill the scaling hypothesis, the values of the maxima in ϕ_n scale as $L^{1/\nu}$: $\phi_n^{\max}(L) \propto L^{1/\nu}$. The exponent (γ/ν) can be calculated without knowing T_C from the scaling behavior of the maximum of the susceptibility: $\chi^{\max}(L) \propto L^{\gamma/\nu}$. The relations between the critical and the effective temperatures $T_C^{\mathcal{K}}(L)$, $T_C^{\phi_n}(L)$ have the same form. For instance, in the case of the susceptibility, we can write

$$T_C^{\mathcal{K}}(L) = T_C + \mathcal{F}_{\mathcal{K}} L^{-1/\nu}, \quad (7)$$

where $\mathcal{F}_{\mathcal{K}}$ is a constant. The critical temperature T_C can be calculated from this relation, provided that ν is known.

An alternative method to determine T_C , without knowing ν has been introduced by Binder.²⁶ The fourth order magnetization cumulant reads

$$U(L,T) = 1 - \frac{\langle M^4 \rangle_T}{3\langle M^2 \rangle_T^2}. \quad (8)$$

In translation invariant lattices, $U(L,T)$ exhibits a fixed point at $T=T_C$: $U(L,T_C) = U^*$, where U^* is an universal value, independent on the system size.

It should be emphasized that in the case of fractals, the values of L we investigate are not uniformly distributed since they define a geometrical series with a ratio b ; the incrementation of a segmentation step has a very high computation cost and strongly reduces the efficiency of the histogram method by increasing L very quickly. Since laws have to be fitted from a low number of points, although they are distributed in a large range of sizes, one must remain very careful. For every fit, we performed a classical least square (LS) linear method and a nonlinear fit based upon a steepest descent method [Levenberg-Marquardt algorithm].²⁷ The latter method gives a more important weight to the points calculated when L is large; small differences appear between the two fits when studying the maxima of the susceptibility, slightly enlarging some error bars. The reliability coefficient R^2 of a fit is defined as the square of the Pearson correlation coefficient related to the classical "chi square" method.²⁷

III. NUMERICAL RESULTS

In this section, we have revisited SC(3,1) by increasing the segmentation step to 8 ($L=6561$). Moreover, we have investigated the cases SC(5,1), SC(4,2), and SC(5,3).

A. Fractal SC(5,1): $d_f \approx 1.9746$

Four segmentation steps from $k=2$ to $k=5$ have been investigated in the case of SC(5,1). When processing the data of several Monte Carlo runs at a given temperature, one can notice that the reliability of the histogram method depends not only upon k , but also upon the thermodynamic average considered. In a more general way, the precision is always better when considering the magnetization, the sus-

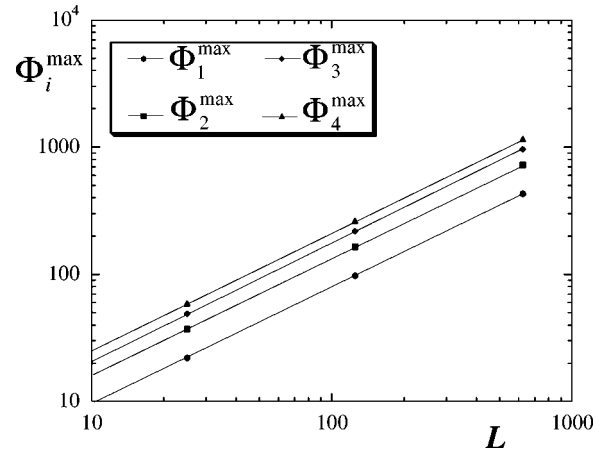


FIG. 2. The maxima of the logarithmic derivatives Φ_n^{\max} , from $k=2$ to $k=4$, versus the size L , for SC(5,1).

ceptibility or the Binder cumulant than in the case of the logarithmic derivatives or the specific heat. As a result, we were able to compute the maxima of the logarithmic derivatives Φ_n^{\max} and the positions of the associated effective temperatures $T_C^{\Phi_i}(L)$ from $k=2$ to $k=4$ only. The values of these maxima are plotted as a function of L in Fig. 2. As for the next figures, the error bars associated with statistical uncertainties are smaller than the size of the dots, if they are not plotted. No finite size scaling corrections can be brought out from these data, since the laws $\Phi_n^{\max}(L) \sim L^{1/\nu}$ are satisfied by each of the four fits with reliability coefficients $R^2 = 1.00000$ and lead to a mean value $\nu = 1.083 \pm 0.002$.

The effective critical temperatures $T_C^{\Phi_i}(L)$ are plotted in Fig. 3 as a function of $L^{-1/\nu}$, with $\nu = 1.083$. The behavior expected from finite size scaling is satisfied with reliability coefficients $R^2 > 0.99980$ for each fit, and ν varying from 1.081 to 1.085. The ordinates at the origin lie in a range between 2.0635 and 2.0665, yielding $T_C = 2.0650 \pm 0.0015$.

As an alternative method to determine the critical temperature, we studied the behavior of the Binder cumulant as a function of the temperature for k varying from 2 to 5; the

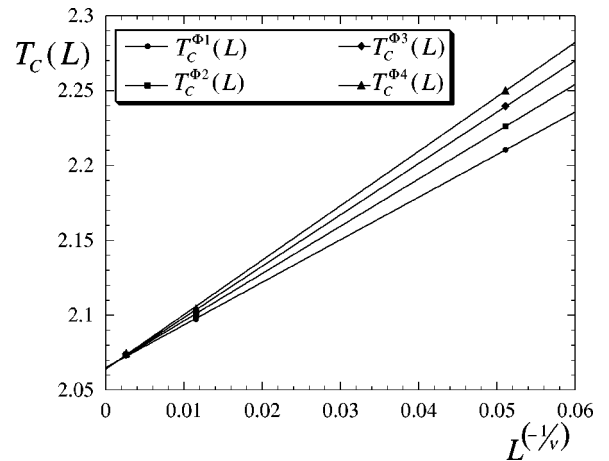


FIG. 3. The effective critical temperatures $T_C^{\Phi_i}(L)$ versus $L^{-1/\nu}$, with $\nu = 1.083$, for SC(5,1).

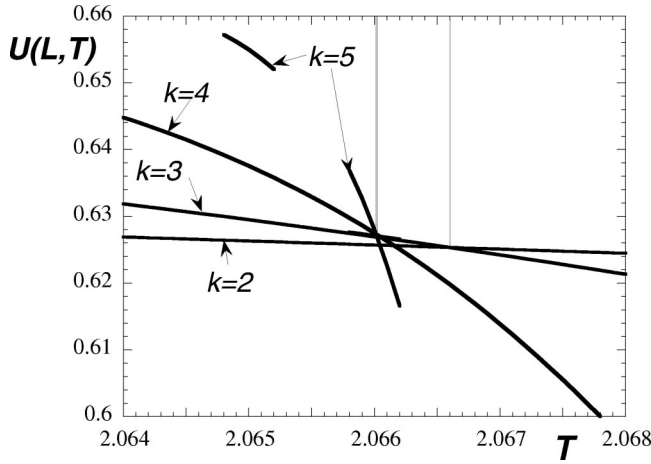


FIG. 4. The Binder cumulant versus the temperature for $k=2$ to 5, for SC(5,1).

results of our simulations are plotted in Fig. 4. The coordinates of the intersection points between a segmentation step and the following are summarized in Table I. As already pointed out in our previous paper, the curves do not exactly intersect at a fixed point. This effect is much less important in the present case than for SC(3,1): the convergence is faster and the relative variation of temperature separating the two last points is about 10^{-5} , yielding $T_C=2.0660$. This value lies within the error bars provided by the first method. We thus performed several Monte Carlo runs between $T_C=2.0650$ and $T_C=2.0660$, in order to explore the range of temperature provided by the calculation of T_C . The magnetization and the susceptibility are plotted as a function of L in Figs. 5 and 6. Their finite size behavior is very sensitive to the value of the temperature when L is large, since the transition is narrowed down as L increases. The cumulant crossing method yields the most precise value of the critical temperature; the laws $m \sim L^{-\beta/\nu}$ and $\chi \sim L^{\gamma/\nu}$ are satisfied in the best way by two fits (respectively three and four points) for the same temperature $T_C=2.0660$, both with reliability coefficients $R^2=1.00000$. They yield with four sizes from $L=25$ to $L=3125$, $\beta/\nu=0.1106(4)$, and $\gamma/\nu=1.743(5)$; with three sizes from $L=125$ to $L=3125$, $\beta/\nu=0.1108(4)$, and $\gamma/\nu=1.750(5)$. These fits are very stable, in agreement within their error bars, and cover several orders of magnitude. They are consistent with the estimations of T_C from the behavior of $T_C^{\Phi_i}(L)$ and thus the estimation of ν from the

TABLE I. Temperatures of the cumulant crossing points between a step and the next one. The error bars are of one integer on the last digit.

d_f	1.9746	1.8927	1.7925	1.7227
$(k=2 \leftrightarrow k=3)$	2.06660			0.8931
$(k=3 \leftrightarrow k=4)$	2.06604		1.0917	0.8372
$(k=4 \leftrightarrow k=5)$	2.06602	1.48570	1.0649	0.8075
$(k=5 \leftrightarrow k=6)$		1.48154	1.0490	
$(k=6 \leftrightarrow k=7)$		1.48012		

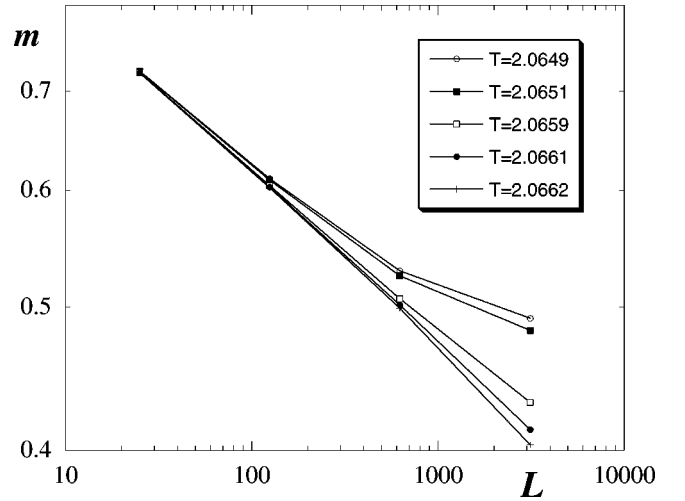


FIG. 5. The magnetization versus L , for SC(5,1), for several values of the simulation temperature in the critical region.

behavior of $\Phi_n^{\max}(L)$. In order to ensure that the convergence towards the infinite limit is reached, we disregarded the second segmentation step; in this way, we eliminate systematic errors leading to slightly underestimations of the values of the exponents β/ν and γ/ν .

As a conclusion we have $\beta/\nu=0.1108(4)$ and $\gamma/\nu=1.750(5)$. The Rushbrooke and Josephson scaling law $d_{\text{eff}} = \gamma/\nu + 2(\beta/\nu)$ is satisfied with an effective dimension $d_{\text{eff}}=1.9716 \pm 0.0058$. The relative difference between d_{eff} and the Hausdorff fractal dimension $d_f=1.9746$ is smaller than 0.2%. No straight evidence for a discrepancy between these dimensions can be brought out from these results: As already showed in the case of fractal dimensions between two and three,¹⁶ the hyperscaling relation is satisfied with $d_{\text{eff}}=d_f$.

The exponent α deduced from the Rushbrooke scaling law²³ $\alpha=2-2\beta-\gamma$ leads to the negative value $\alpha=-0.14 \pm 0.018$. As already noticed in Sec. II, the specific heat ex-

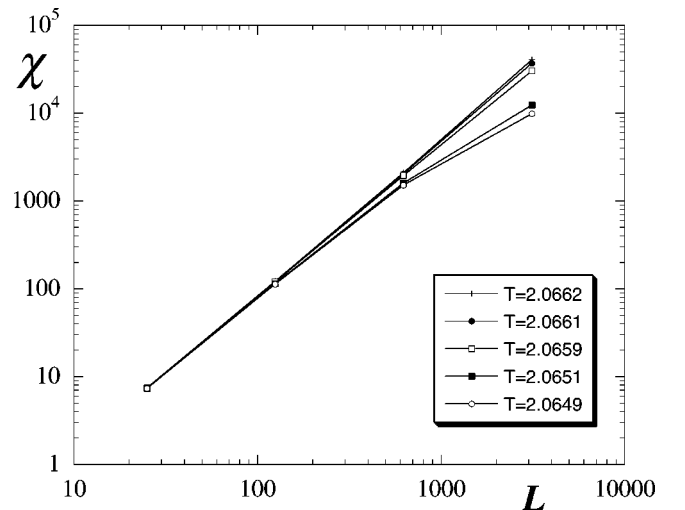


FIG. 6. The susceptibility versus L , for SC(5,1), for several values of the simulation temperature in the critical region.

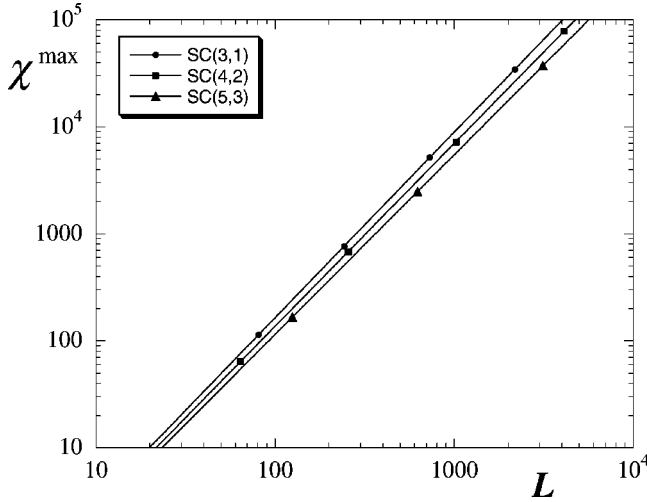


FIG. 7. The maxima of the susceptibility $\chi^{\max}(L)$ versus L , for SC(3,1), SC(4,2), and SC(5,3).

hibits a humplike behavior $C(L, T) = C_{\infty}(t) + L^{\alpha/\nu} C(tL^{1/\nu})$. We cannot extract (α/ν) in a reliable way from a fit involving that relation. Nevertheless, assuming that $\alpha = -0.140$ and $\nu = 1.083$ we find from a three points fit that $C(L, T_C = 2.0660) = 4.1 - 4.1 \cdot L^{-0.129}$ with a good reliability $R^2 = 0.99983$.

B. Fractal SC(3,1): $d_f \approx 1.8927$

This case has been extensively studied in Monceau *et al.*¹³ and Carmona *et al.*¹⁴ Additional simulations enabled us to calculate the cumulant crossing point between the sixth and the seventh iteration steps and to study the behavior of m and χ in the range of the estimated critical temperature at the eighth iteration step. Moreover, we studied the behavior of the maxima of the susceptibility $\chi^{\max}(L)$ as an alternative method to determine (γ/ν) .

The maxima of the susceptibility $\chi^{\max}(L)$ are plotted in Fig. 7 as a function of L ; we check that the law $\chi^{\max}(L) \sim L^{\gamma/\nu}$ is very well satisfied by the LS fits with a reliability coefficient $R^2 = 1.00000$. They yield with three sizes from $L = 81$ to $L = 729$, $\gamma/\nu = 1.735(3)$; with four sizes from $L = 81$ to $L = 2187$, $\gamma/\nu = 1.733(4)$; with five sizes: from $L = 81$ to $L = 6561$, $\gamma/\nu = 1.733(4)$; with three sizes: from $L = 729$ to $L = 6561$, $\gamma/\nu = 1.732(4)$. A five points LM fit yields $\gamma/\nu = 1.730(1)$.

The stability of these power law fits, with data covering several orders of magnitude is one of the most striking results of the simulations we carried out: Unlike Carmona and co-workers,¹⁴ it turns out that a scaling correction exponent ω , cannot be extracted from the behavior of $\chi^{\max}(L)$ in a reliable way. We are able to retain that $(\gamma/\nu) = 1.732(4)$. The result we calculated in our first paper¹³ by fitting the susceptibility as a function of the size at the expected critical temperature is slightly higher than the present one: we found $(\gamma/\nu) = 1.76(1)$. The relative difference of about 2% between these values is induced by the uncertainty about the critical temperature. We are now able to go back over these results.

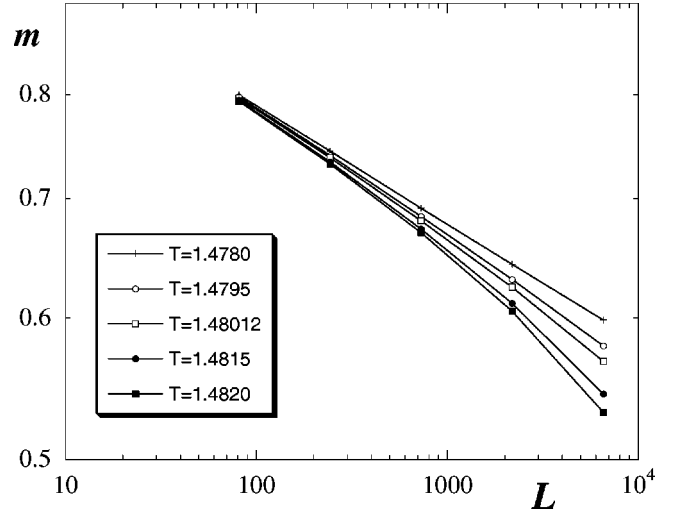


FIG. 8. The magnetization versus L , for SC(3,1), for several values of the simulation temperature in the critical region.

The behaviors of $\chi(L)$ and $m(L)$ with T as a parameter are plotted in Figs. 8 and 9 for the five values of k between 4 and 8. As the temperature decreases from 1.4820, the points tend to line up along straight lines for the two averages simultaneously. Moreover, a close look at Table I shows clearly that the convergence of cumulant crossing points towards the infinite limit value of the temperature is much slower than in the case of SC(5,1). These observations lead to think that the values of the critical temperatures announced in Monceau *et al.*¹³ (1.482 ± 0.0015) and Carmona *et al.*¹⁴ (1.4812 ± 0.0002) are slightly overestimated. It already appears from the comparison between SC(5,1) and SC(3,1) that a contribution to scaling corrections arises from the slow convergence of the transition towards the thermodynamical limit with L in the latter case. This convergence speed can be related to the behavior of the mean number of nearest neighbors per site $\langle z(b, c, k) \rangle$ with k for a given fractal dimension: Fig. 1 shows that the convergence of $\langle z(b, c, k) \rangle$ is slower in the case of SC(3,1) than SC(5,1).

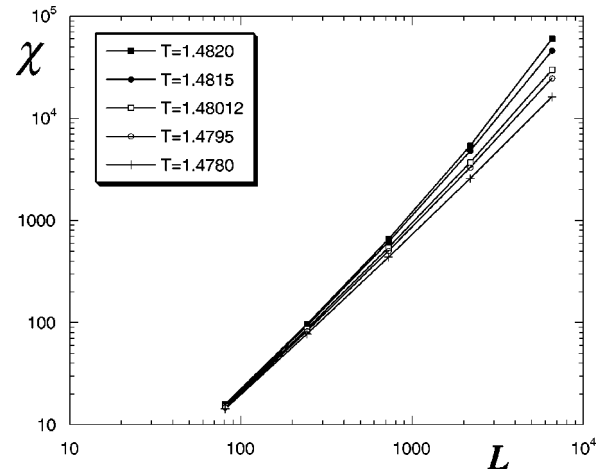


FIG. 9. The susceptibility versus L , for SC(3,1), for several values of the simulation temperature in the critical region.

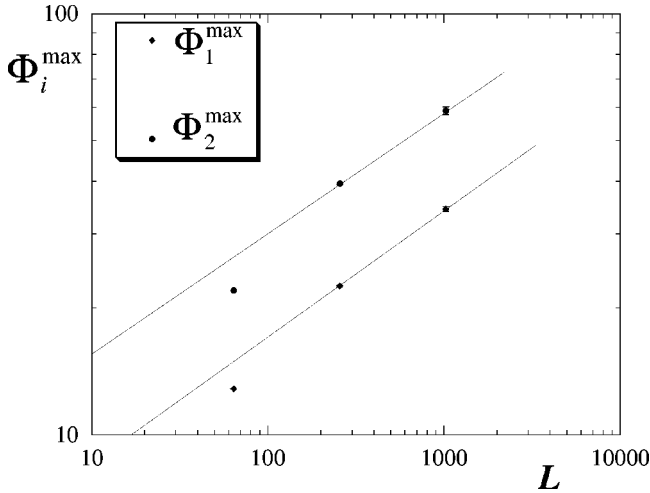


FIG. 10. The values of the maxima of the logarithmic derivatives Φ_1^{\max} and Φ_2^{\max} versus the size L from $k=3$ to $k=5$, for SC(4,2).

Strong difficulties arise from the uncertainty about T_C in analyzing the critical behavior. When taking into account classical scaling corrections, we should look for a finite size behavior of the magnetization (for instance) following the usual classical expression $m \sim L^{-\beta/\nu}(1 + A_m L^{-\omega})$, right at T_C . Since the value of the critical temperature is not accurate enough, and the number of points small, we cannot fit such an expression directly in a reliable way. Moreover, the lack of translation invariance is also related to the scaling corrections: we deal with fractal networks, where the local connectivity is not homogeneous, and where the holes size distribution covers several orders of magnitude. As a matter of fact, for a fixed value of b , the study of SC(5,3) will show that the fractal dimension has a strong influence on scaling corrections. Thus they are not only caused by a classical finite size effect, but they have a topological origin too; there is no strong evidence that they can be described properly with a $L^{-\omega}$ term. Nevertheless, an estimation of β/ν can be provided in the following way: we retain as an estimate of the critical temperature the one which yields a value of γ/ν as close as possible of the result provided by the scaling of $\chi^{\max}(L)$; we find $T=1.4795$, where a four points fit yields $\chi(L) \sim L^{-1.73}$ with a reliability coefficient $R^2=0.99980$. We perform then a four points fit of $m(L)$ at $T=1.4795$ as a function of $L^{-\beta/\nu}$; it yields $\beta/\nu=0.0743$ with $R^2=0.99950$. The uncertainty about the critical temperature, and the slowly vanishing scaling corrections lead to systematical er-

TABLE II. Effective temperatures of the maxima of the thermodynamic derivatives and the susceptibility for SC(4,2). The error bars are of one integer on the last digit.

L	$T_C^\chi(L)$	$T_C^{\Phi_1}(L)$	$T_C^{\Phi_2}(L)$
64	1.34798	1.38985	1.40392
256	1.23971	1.26057	1.27274
1024	1.17850	1.18430	1.18506
4096	1.13880		

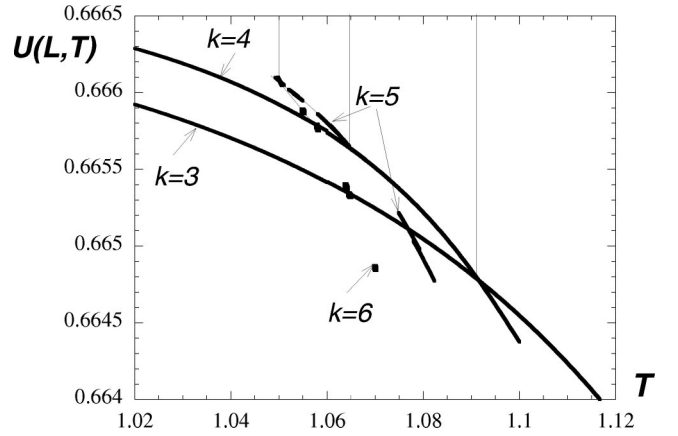


FIG. 11. The variations of the Binder cumulant $U(L, T)$ versus T , for SC(4,2).

rors, enlarging the error bar about β/ν . By sweeping the interval around $T=1.4795$, we can estimate that $\beta/\nu = 0.075 \pm 0.01$. These results yield $d_{\text{eff}} = \gamma/\nu + 2(\beta/\nu) = 1.882 \pm 0.024$. No significant deviation from the fractal dimension in the hyperscaling relation can be brought out from these results. A lower bound for ν can be calculated from the behavior of the logarithmic derivatives. The set of critical parameters or their associated bounds are reported in Tables IV and V.

C. Fractal SC(4,2): $d_f \approx 1.7925$

Four segmentations steps have been studied, from $k=3$ to $k=6$. The values of the maxima of the logarithmic derivatives Φ_1^{\max} and Φ_2^{\max} are plotted as a function of the size L from $k=3$ to $k=5$ in Fig. 10. Since the location of these maxima for $k=5$ needed huge amount of Monte Carlo runs, we did not to calculate the less precise peaks Φ_3^{\max} and Φ_4^{\max} . The values of Φ_1^{\max} and Φ_2^{\max} at the fifth iteration step have been extracted from two independent histograms of 3 millions steps independently by each of us. It is worth noticing

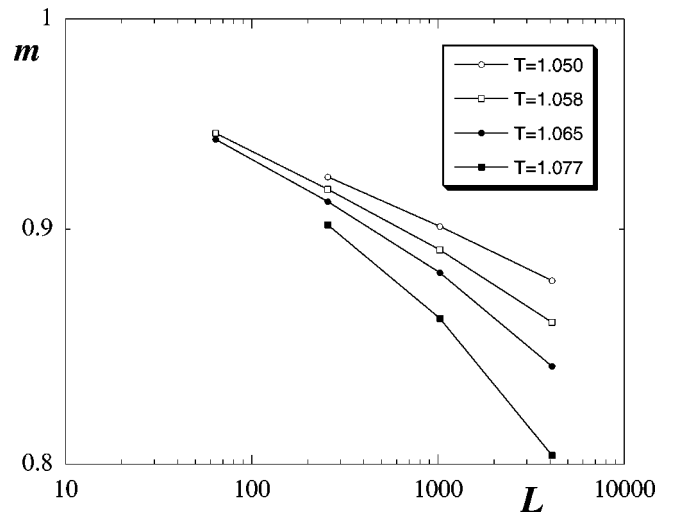


FIG. 12. The magnetization versus L , for SC(4,2), for several values of the simulation temperature in the critical region.

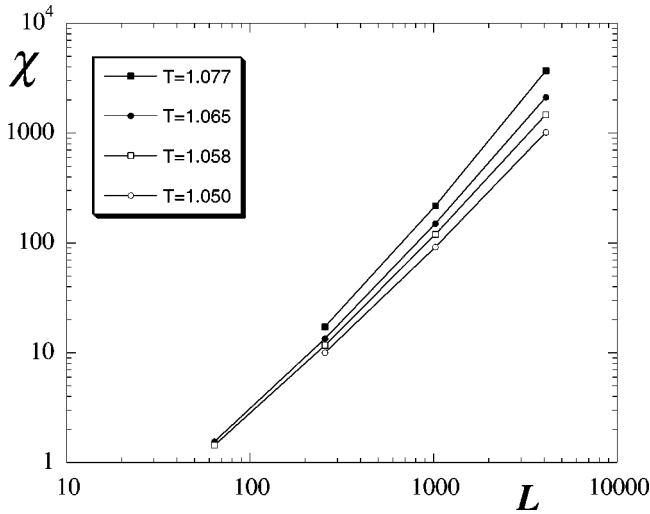


FIG. 13. The susceptibility versus L , for SC(4,2), for several values of the simulation temperature in the critical region.

that scaling corrections appear to be very important even at the third iteration step. The value extracted from a fit of the fourth and the fifth iteration steps yields $\nu=3.37(20)$. The values of the effective critical temperatures $T_C^{\Phi_i}(L)$ and $T_C^\chi(L)$ are summarized in Table II. The agreement between these values and the results of Carmona *et al.* is good, within a relative precision better than 0.1%.

We performed several fits of these temperatures as a function of $L^{-1/\nu}$ with ν varying from 3.1 to 3.6. The ordinates at the origin extracted from $T_C^{\Phi_1}(L)$ and $T_C^{\Phi_2}(L)$ (only the steps $k=4$ and $k=5$ can be taken in account) do not intersect at the same point, and lie in a range between 1.00 and 1.03. On the other hand the behavior of $T_C^\chi(L)$ expected from finite size scaling is obeyed with good reliability coefficients (>0.9999) for three segmentation steps and ν varying from 3.1 to 3.50. The associated critical temperatures extracted from these last fits lie in a range between 1.07 and 1.05. As a conclusion of these fits, the logarithmic derivatives suffer

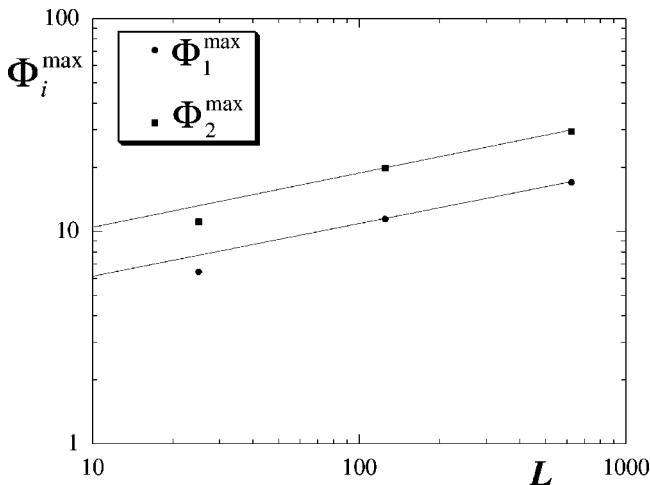


FIG. 14. The maxima of Φ_1^{\max} and Φ_2^{\max} versus L from $k=2$ to $k=4$, for SC(5,3).

TABLE III. Effective temperatures of the maxima of the thermodynamic derivatives and the susceptibility for SC(5,3). The error bars are of one integer on the last digit.

L	$T_C^\chi(L)$	$T_C^{\Phi_1}(L)$	$T_C^{\Phi_2}(L)$
25	1.39440	1.49802	1.53130
125	1.15764	1.20173	1.21550
625	1.03632	1.06117	1.06378
3125	0.96110		

from larger scaling corrections than the susceptibility. The value 3.37 extracted from the finite size behavior of Φ_i^{\max} provides only a lower bound for the correlation length exponent ν .

The intersection points of the Binder cumulants between a segmentation step and the following are summarized in Table I, and the variations of $U(L, T)$ with T plotted in Fig. 11. It appears clearly that the convergence of the temperature is much slower than in the two previous cases SC(5,1) and SC(3,1).

Figure 7 shows the behavior of $\chi^{\max}(L)$ as a function of L . The relation $\chi^{\max}(L) \sim L^{\gamma/\nu}$ is satisfied by two LS fits (respectively, three and four points), both with a reliability coefficient $R^2=1.00000$. They yield with three sizes from $L=64$ to $L=1024$, $\gamma/\nu=1.702(5)$; with four sizes from $L=64$ to $L=4096$, $\gamma/\nu=1.708(5)$; with three sizes from $L=256$ to $L=4096$, $\gamma/\nu=1.713(4)$.

A three points LM fit yields 1.72. As in the case of SC(3,1), we notice once again the very robust character of the power laws fitted from $\chi^{\max}(L)$; we are able to retain the value $\gamma/\nu=1.71(1)$. The relative difference between the value obtained by Carmona and co-workers [1.67(2)] and ours is smaller than 2.5%. The size of the error bars does not enable to conclude that there is a significant discrepancy between the results of the two groups.

We have reached a stage where the critical region can be studied. We performed several Monte Carlo runs in the range of temperature between 1.050 and 1.077. The magnetization and the susceptibility are plotted as a function of L in Figs.

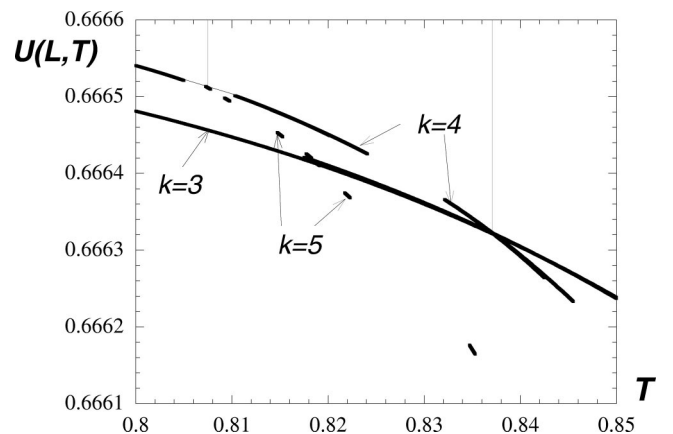


FIG. 15. The variations of the Binder cumulant $U(L, T)$ versus T , for SC(5,3).

TABLE IV. The critical temperatures and critical exponents on SC(3,1), SC(4,2), SC(5,1), and SC(5,3) following Monceau *et al.*, Carmona *et al.*, and the present work (k is the highest value of the segmentation step taken in account)

Author	Fractal	Fractal dimension	T_c	$\frac{\beta}{\nu}$	$\frac{\gamma}{\nu}$	d_{eff}	Boundary conditions	k
This work	SC(5,1)	1.9746	2.0660(15)	0.1108(4)	1.750(5)	1.9716(58)	periodic	5
Monceau <i>et al.</i> (Ref. 13)	SC(3,1)	1.8927	1.482(15)	0.0815(30)	1.76(1)	1.923(16)	periodic	7
Carmona <i>et al.</i> (Ref. 14)	SC(3,1)	1.8927	1.481	0.080(1)	1.730(1)	1.890(2)	periodic	7
Monceau <i>et al.</i> (Ref. 13)	SC(3,1)	1.8927	1.481	0.147(4)	1.625(20)	1.919(28)	free	7
This work	SC(3,1)	1.8927	1.4795(5)	0.075(10)	1.732(4)	1.882(24)	periodic	8
Carmona <i>et al.</i> (Ref. 14)	SC(4,2)	1.7925	1.077	0.069(10)	1.67(2)	1.81(3)	periodic	6
This work	SC(4,2)	1.7925	<1.049		1.71(1)	>1.70	periodic	6
This work	SC(5,3)	1.7227	<0.808		1.683(5)	>1.678	periodic	5

12 and 13. It appears than the critical temperature calculated in Carmona *et al.*¹⁴ ($T_c = 1.0776$) is slightly overestimated: as the temperature decreases from 1.077 to 1.050 the points tend to line up along straight lines for the two averages simultaneously. These behaviors are consistent with the upper bound value of the critical temperature extracted from the Binder cumulants: $T_c < 1.0490$. The arguments set out at the end of the last section prevent us from fitting scaling corrections in a reliable way and thus from estimating β/ν in the present case.

D. Fractal SC(5,3): $d_f \approx 1.7227$

As for SC(5,1), four segmentation steps, from $k=2$ to $k=5$, have been investigated in the case of SC(5,3). The comparison between these two fractals is very interesting, because they share the same values of b , thus the same series of sizes, but they have different fractal dimensions. The values of the maxima Φ_1^{max} and Φ_2^{max} are plotted as a function of L from $k=2$ to $k=4$ in Fig. 14. Unlike the case of SC(5,1), scaling corrections have an important effect at the second iteration step. As a result of this, it appears clearly that, in the case of a fractal network, these corrections are strongly related to the fractal dimension. A fit from the third and the fourth iteration step, yields $\nu = 4.06(20)$. From the effective critical temperatures $T_c^{\Phi_i}(L)$ and $T_c^\chi(L)$ reported in Table III, we performed several fits as a function of $L^{-1/\nu}$ with ν vary-

ing from 3.8 to 4.3. The ordinates at the origin extracted from $T_c^{\Phi_1}(L)$ and $T_c^{\Phi_2}(L)$ do not intersect at the same point, and lie in a range between 0.73 and 0.79; the behavior of $T_c^\chi(L)$ expected from finite size scaling is obeyed with lower reliability coefficients than in the case of SC(4,2) for three segmentation steps and L varying from 125 to 3125; the associated critical temperatures lie in a range between 0.812 and 0.788. These discrepancies in the estimations of the critical temperatures show that scaling corrections affect ϕ_1 , and ϕ_2 with different and large amplitudes. As for SC(4,2), the value 4.06 extracted from the finite size behavior of Φ_i^{max} provides only a lower bound for ν .

The behavior of the Binder cumulant, plotted in Fig. 15, has to be compared with SC(5,1): The associated crossing points, reported in Table I, show clearly the effects of the fractal dimension on finite size scaling. Besides strong scaling corrections already mentioned above, one observes a slowing down of the convergence of the intersections points of the Binder cumulant with k towards the infinite limit as the fractal dimension decreases. It is striking that this slowing down is reflected in the variations of $\Delta z(b, c, k)$ with k plotted in Fig. 1, for the four values of the fractal dimensions studied in this paper. As a result, we should be led to disregard the third iteration step from our fits, since it is obviously still too far from the asymptotic limit. The two last crossing points of $U(L, T)$ are 0.8080 and 0.8188. The relative differ-

TABLE V. The critical exponents on SC(3,1), SC(4,2), SC(5,1), and SC(5,3) following Monceau *et al.*, Carmona *et al.*, and the present work (following)

Author	Fractal	ν	β	γ	Boundary conditions
This work	SC(5,1)	1.083(3)	0.120(4)	1.90(1)	periodic
Monceau <i>et al.</i> (Ref. 13)	SC(3,1)	1.565(10)	0.127(6)	2.754(25)	periodic
Carmona <i>et al.</i> (Ref. 14)	SC(3,1)	1.70(1)	0.1360(25)	2.94(2)	periodic
Monceau <i>et al.</i> (Ref. 13)	SC(3,1)	1.73(3)	0.254(11)	2.81(8)	free
This work	SC(3,1)	>1.565	>0.11	>2.70	periodic
Carmona <i>et al.</i> (Ref. 14)	SC(4,2)	3.23(8)	0.223	5.39	periodic
This work	SC(4,2)	>3.37		>5.73	periodic
This work	SC(5,3)	>4.06		>6.81	periodic

ence is so large that we are obviously still too far from the asymptotic critical temperature to calculate β/ν ; we are able to retain 0.8080 as an upper bound for the critical temperature.

Figure 7 shows the behavior of the maximum of the susceptibility $\chi^{\max}(L)$ as a function of L . As in the previous cases, the relation $\chi^{\max}(L) \sim L^{\gamma/\nu}$ is very well satisfied by a three points LS fit (with a reliability coefficient $R^2 = 1.00000$): with three sizes from $L=125$ to $L=3125$, $\gamma/\nu = 1.678(5)$; with two sizes from $L=625$ to $L=3125$, $\gamma/\nu = 1.683(5)$. A LM fit yields $\gamma/\nu = 1.683(1)$. We are able to conclude that $\gamma/\nu = 1.683(5)$.

IV. DISCUSSION

The results summarized in Table I show that the differences between two successive intersections of the cumulant crossing points, much larger than the precision of our numerical computations, are no more compatible with the existence of a fixed point over a large range of finite scales. However, the values of these crossing points converge towards a finite nontrivial value which can be considered as the critical temperature of the mathematical fractal, as $k \rightarrow \infty$. As a consequence, the estimations of T_C based upon the successive positions of these intersection points are overestimated. The block size calculations of Binder²⁶ implicitly assume the translation invariance of the structure, when making the hypothesis that all finite size blocks are identical. In the case of fractal structures, the blocks are the successive finite segmentation structures; it is obvious that they are far from being identical. Although they exhibit self-similarity, topological properties change from a step k to the following. This can be easily seen by looking for instance at the evolution of $\Delta z(b, c, k)$ with k plotted in Fig. 1. Discrepancies with the standard finite size scaling analysis when k is low can be explained not only by a pure finite-size effect, but also by a topological contribution to scaling corrections. The comparison between the results obtained for SC(5,1) and SC(5,3) confirms the topological nature of these scaling corrections: the sizes L are in a geometrical series with the same ratio b , and the deviation from expected power laws is much more important in the latter case. We can expect from the results obtained in the four cases we investigated that, for a given set of values of b and c , the topological scaling corrections can be neglected, provided that k is large enough. It clearly occurs for SC(5,1) where the consistency of the finite size scaling analysis is very good, provided that $L > 25$; it is precisely in this latter case that we can observe a quicker convergence of $\langle z(b, c, k) \rangle$ towards his limit as $k \rightarrow \infty$.

Since the fixed point of the Binder cumulants is replaced by a sequence of intersection points, the critical temperature is the limit of that sequence as $k \rightarrow \infty$. This behavior is quite similar to the one observed in the study of percolation by renormalization methods in random fractals.²⁸ Binder himself noticed that the topology of the blocks has a strong influence on their distribution function. He pointed out that, since the correlation length tends towards infinity at the criti-

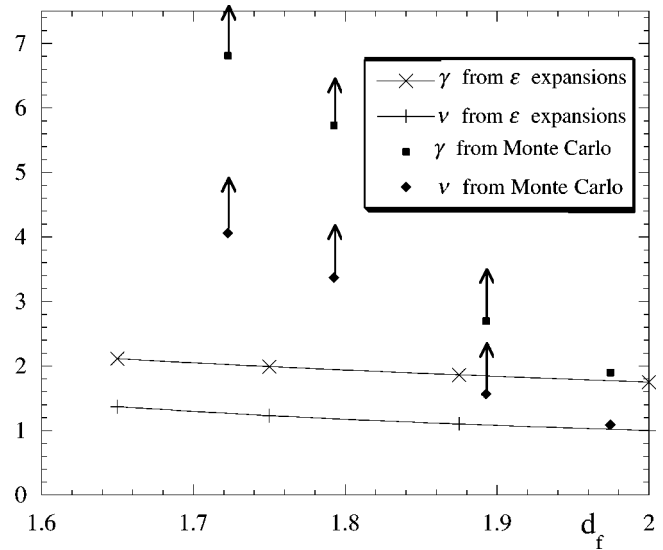


FIG. 16. Comparison between the exponents γ and ν provided by ϵ expansions and Monte Carlo; the arrows indicate that the associated points are lower bounds.

cal temperature, the effect of boundary conditions can never be completely neglected, even if the size of the blocks becomes very large. This is related to the observation of a different set of critical exponents between periodic boundary conditions and free edges in Monceau *et al.*¹³ summarized in Tables IV and V.

A more precise study of the mean local connectivity of Random Sierpinski carpets has been carried out by Lévy and Perreau;¹⁹ transfer-matrix methods allowed them to show in an analytical way that fractal subdimensions appear besides the Hausdorff dimension. These subdimensions, which are indeed scaling corrections and remain present in the deterministic case, can be brought out from numerical simulations of the local connectivity,²⁹ but are very difficult to detect experimentally.³⁰ We can assume that these fractal subdimensions are related to the scaling corrections that Carmona *et al.* and we brought out from the magnetic behavior of Sierpinski carpets.

The critical exponents or their associated bounds are reported in Tables IV and V; Fig. 16 shows the values of the exponents ν and γ provided by ϵ expansions,⁸ and the values (or the bounds) we provide in the present work. The discrepancies between the values of the exponents provided by ϵ expansions and Monte Carlo simulations increase as the fractal dimension decreases (below 2).

ACKNOWLEDGMENTS

A part of numerical simulations has been carried out in the national center of computational resources IDRIS, supported by the CNRS (Project No. 991186). We acknowledge the scientific committee and the staff of the center. We are also grateful to the research computational center (CCR) of the Université Paris VII-Denis-Diderot, where the rest of the simulations have been done.

- ¹Y. Gefen, B.B. Mandelbrot, and A. Aharony, Phys. Rev. Lett. **45**, 855 (1980).
- ²Y. Gefen, A. Aharony, and B. Mandelbrot, J. Phys. A **16**, 1267 (1983).
- ³Y. Gefen, Y. Meir, B.B. Mandelbrot, and A. Aharony, Phys. Rev. Lett. **50**, 145 (1983).
- ⁴Y. Gefen, A. Aharony, Y. Shapir, and B. Mandelbrot, J. Phys. A **17**, 435 (1984).
- ⁵Y. Gefen, A. Aharony, and B. Mandelbrot, J. Phys. A **17**, 1277 (1984).
- ⁶J.R. Ding, and B.X. Liu, Phys. Rev. B **40**, 5834 (1989).
- ⁷B. Bonnier, Y. Leroyer, and C. Meyers, Phys. Rev. B **37**, 5205 (1988).
- ⁸J.C. Le Guillou and J. Zinn-Justin, J. Phys. (France) **48**, 19 (1987).
- ⁹B. Bonnier, Y. Leroyer, and C. Meyers, Phys. Rev. B **40**, 8961 (1989).
- ¹⁰G. Bhanot, D. Duke and R. Salvador, Phys. Lett. **165B**, 355 (1985).
- ¹¹B. Bonnier, Y. Leroyer, and C. Meyers, J. Phys. (Paris) **48**, 553 (1987).
- ¹²J.C. Angles d'Auriac and R. Rammal, J. Phys. A **19**, L655 (1986).
- ¹³P. Monceau, M. Perreau, and F. Hébert, Phys. Rev. B **58**, 6386 (1998).
- ¹⁴J. Carmona, U.M.B. Marconi, J.J. Ruiz-Lorenzo, and A. Tarancon, Phys. Rev. B **58**, 14 387 (1998).
- ¹⁵S.H. Liu, Phys. Rev. B **32**, 5804 (1985).
- ¹⁶P.Y. Hsiao, P. Monceau, and M. Perreau, Phys. Rev. B **62**, 13 856 (2000).
- ¹⁷D. Ledue, D.P. Landau, and J. Teillet, Phys. Rev. B **51**, 12 523 (1995).
- ¹⁸B. B. Mandelbrot, *Fractals: Form, Chance and Dimension* (Freeman, New York, 1977).
- ¹⁹M. Perreau and J.C.S. Levy, Phys. Rev. A **40**, 4690 (1989).
- ²⁰U. Wolff, Phys. Rev. Lett. **60**, 1461 (1988).
- ²¹A.M. Ferrenberg and R.H. Swendsen, Phys. Rev. Lett. **61**, 2635 (1988).
- ²²A.M. Ferrenberg and R.H. Swendsen, Phys. Rev. Lett. **63**, 1195 (1989).
- ²³M.E. Fisher, in *Critical Phenomena*, edited by M.S. Green (Academic, New-York, 1971).
- ²⁴M.E. Fisher and M.N. Barber, Phys. Rev. Lett. **28**, 1516 (1972).
- ²⁵A.M. Ferrenberg and D.P. Landau, Phys. Rev. B **44**, 5081 (1991).
- ²⁶K. Binder, Z. Phys. B: Condens. Matter **43**, 119 (1981).
- ²⁷W.H. Press, B.P. Flannery, S.A. Teukolsky, and W.T. Vetterling, in *Numerical Recipes, the Art of Scientific Computing* (Cambridge University Press, Cambridge, 1986).
- ²⁸M. Perreau, J. Peiro, and S. Berthier, Phys. Rev. E **54**, 4590 (1996).
- ²⁹P. Monceau and J.C.S. Lévy, Phys. Lett. A **171**, 167 (1992).
- ³⁰D. Berger, S. Chamaly, M. Perreau, D. Mercier, P. Monceau, and J.C.S. Lévy, J. Phys. I **1**, 1433 (1991).